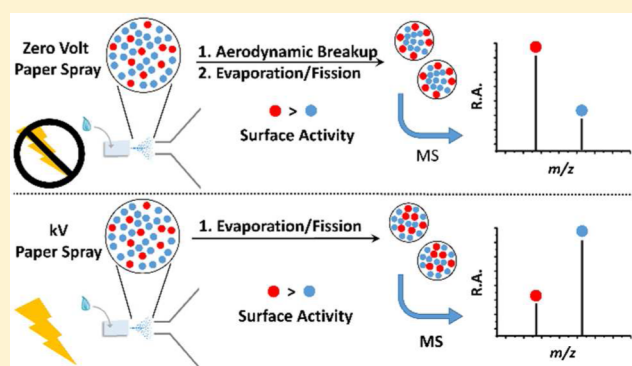


Zero Volt Paper Spray Ionization and Its Mechanism

Michael Wlekinski,^{†,‡} Yafeng Li,^{†,‡} Soumabha Bag,[†] Depanjan Sarkar,[‡] Rahul Narayanan,[‡] T. Pradeep,[‡] and R. Graham Cooks^{*,†}[†]Department of Chemistry and Center for Analytical Instrumentation Development, Purdue University, West Lafayette, Indiana 47907, United States[‡]DST Unit of Nanoscience (DST UNS) and Thematic Unit of Excellence (TUE), Department of Chemistry, Indian Institute of Technology Madras, Chennai, Tamil Nadu 600 036, India

S Supporting Information

ABSTRACT: The analytical performance and a suggested mechanism for zero volt paper spray using chromatography paper are presented. A spray is generated by the action of the pneumatic force of the mass spectrometer (MS) vacuum at the inlet. Positive and negative ion signals are observed, and comparisons are made with standard kV paper spray (PS) ionization and nanoelectrospray ionization (nESI). While the range of analytes to which zero volt PS is applicable is very similar to kV PS and nESI, differences in the mass spectra of mixtures are interpreted in terms of the more significant effects of analyte surface activity in the gentler zero volt experiment than in the other methods due to the significantly lower charge. The signal intensity of zero volt PS is also lower than in the other methods. A Monte Carlo simulation based on statistical fluctuation of positive and negative ions in solution has been implemented to explain the production of ions from initially uncharged droplets. Uncharged droplets first break up due to aerodynamic forces until they are in the 2–4 μm size range and then undergo Coulombic fission. A model involving statistical charge fluctuations in both phases predicts detection limits similar to those observed experimentally and explains the effects of binary mixture components on relative ionization efficiencies. The proposed mechanism may also play a role in ionization by other voltage-free methods.



Mass spectrometry (MS) is a powerful analytical technique because of its high sensitivity, selectivity, and speed. Ionization, the first step in MS analysis, plays a pivotal role in the experiment. The applicability of MS to complex samples examined without sample pretreatment is the key feature of desorption electrospray ionization (DESI)¹ and other ambient ionization methods.^{2,3} These ionization methods have been used in various fields including drug discovery, metabolomics, forensic science, and biofluid analysis. Ambient ionization methods which avoid the use of a high voltage have obvious advantages, especially for in vivo analysis.⁴

The first voltage-free spray ionization method, thermospray, was developed by Vestal et al. in the 1980s as an interface for LC/MS.^{5,6} In this experiment thermal energy was used to help release solvent and create ionized analytes. A few years later, another important voltage-free spray ionization method (SSI) was introduced by Hirabayashi.^{7,8} In this experiment a high speed gas flow is used to break up the bulk solution into droplets, which go on to evaporate and generate gaseous ions. A variety of compounds^{9–11} can be ionized by SSI, and it has been used for in vivo analysis when combined with ultrasonic aerosolization.⁴ Desorption sonic spray ionization¹² (DeSSI, also referred to as easy ambient sonic-spray ionization, EASI^{13,14}) is another example of a zero voltage spray ionization

method. It represents a particular mode of operation of DESI which removes the high voltage. In SSI and EASI ionization, pneumatic forces play an important role. Another voltage-free ionization method, solvent assisted inlet ionization (SAII) is applicable in LC/MS.^{15–17} Here, as in thermospray, both thermal energy and pneumatic forces appear to contribute to ionization. In addition to these voltage-free spray ionization methods, ultrasound produced by piezoelectric devices has also been used for spray ionization.^{18,19} A low frequency ultrasonicator has been used to analyze biomolecules and monitor organic reactions, reducing background noise by decreasing interference from background electrochemical reactions.^{20,21} In 2013, Chung-Hsuan Chen et al. reported yet another new spray ionization method, Kelvin spray ionization,²² which required no external electric energy, the system itself producing a voltage.

Paper spray (PS), first reported in 2009,²³ has proven practically useful for qualitative and quantitative analysis. The use of paper as the substrate in PS allows ionization of compounds of interest while leaving some of the other

Received: March 11, 2015

Accepted: May 29, 2015

Published: May 29, 2015

components of complex matrices adsorbed to the paper; this feature makes it suitable for the quantification of therapeutic drugs in blood.^{24,25} Paper cut to a sharp point ensures that a kilovolt applied potential will generate an electric field high enough to cause emission of charged analyte-containing solvent droplets; these droplets evaporate and undergo Coulomb explosion and perhaps solvated ion emission to give ESI-like mass spectra.²⁶ A recent variant on the PS method uses paper impregnated with carbon nanotubes as a way to achieve the necessary field strengths while applying only a low voltage.²⁷

We show in this study that by removing the applied voltage entirely, a zero volt form of PS can be performed. This experiment, which is phenomenologically similar to the SAI method, retains the advantages of the paper substrate by allowing complex mixtures to be examined directly without chromatography while removing the electric field and dispensing with the strong pneumatic forces needed in the pneumatically assisted ionization methods of SSI and EASI. In zero volt PS, as in SAI, the vacuum provides a sufficient pneumatic force. Our results demonstrate that zero volt PS gives both positive and negative ions just as does conventional kV PS and nESI, albeit with much lower signal intensities. The reduction in signal intensities roughly parallels that between EASI and DESI. Qualitative mechanisms, which are not fully understood, have been proposed for other zero volt methods, but this paper seeks to develop a quantitative model for zero volt paper spray. Simulations, based on the theory of Dodd,²⁸ have been performed to gain insights into the ionization mechanism. The proposed mechanism includes charge separation during droplet formation due to statistical fluctuations in positive and negative ion distributions¹¹ after aerodynamic droplet breakup as described by Jarrold and co-workers.²⁹ Subsequent solvent evaporation and Coulombic fission processes follow the accepted ESI mechanisms.

EXPERIMENTAL DETAILS

Chemicals and Materials. Deionized water was provided by a Milli-Q Integral water purification system (Barnstead Easy Pure II). Morphine and cocaine were purchased from Cerilliant (Round Rock, Texas). Methanol was from Mallinckrodt Baker Inc. (Phillipsburg, NJ). Deuterated methanol and water were provided by Cambridge Isotope Laboratories (Tewksbury, MA). The paper used as the spray substrate was Whatman 1 chromatography paper (Whatman International Ltd., Maidstone, England). All samples were examined in methanol solution except where noted.

Zero Volt Paper Spray. As is shown in Figure 1, the experimental details of zero volt PS were a little different from those previously reported for kV PS.²³ The choice of paper shape for kV PS is important to generate the required electric fields for ionization; however, the choice of paper shape for zero volt PS is less important than the orientation of the paper relative to the MS inlet. Therefore, a rectangular piece of paper cut to 8 mm × 4 mm and held in place by a toothless alligator clip (McMaster-Carr, USA Part 7236K51) was used, with the center of a straight edge being placed closest to the inlet and on the ion optical axis. This arrangement made it easier to control the distance between the paper and the inlet than in the case of a paper triangle (Figure 1a), increasing the reproducibility of the experiment. A xyz-micrometer moving stage (Parker Automation, USA) was used to set the distance between the front edge of the paper and the MS inlet in the range 0.3 mm to 0.5 mm. A camera (Watec Wat-704R) was used to help in

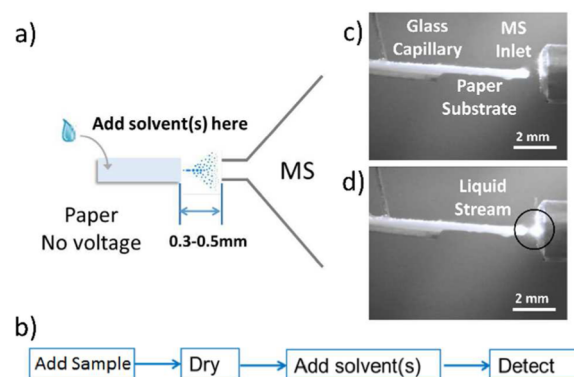


Figure 1. a) Overview of the zero volt paper spray process. The distance between the front edge of the paper and the MS inlet is 0.3–0.5 mm. No voltage is applied to either the paper or the MS inlet capillary. The suction force of the MS inlet causes the release of analyte-containing droplets, which are sampled by the mass spectrometer. b) Sampling and detections procedures. Photographs of the inlet region c) without and d) with solvent. A solvent spray or stream is generated when solvent is applied to the paper, as shown in detail in a video in the Supporting Information.

positioning the paper and to observe the spray which was illuminated by a red laser pointer. No voltage was applied to the paper or the capillary of the MS, instead the spray was generated by the pneumatic forces at play near the MS inlet.

Figure 1b depicts the typical workflow. Typically, 5 μL of sample dissolved in methanol was loaded onto the paper and allowed to dry. During drying, the paper was positioned appropriately with respect to the MS. A methanol and water solvent (1:1 v/v, applied to the paper in three 7 μL aliquots) was used to generate the spray and detect signal. For each 7 μL aliquot of solvent, the signal lasted for about 10 s. Micropipette tips were used to load solvent onto the paper. Sample solutions could also be directly applied to the paper to generate spray. Figures 1c and 1d are photographs taken without and with solvent on the paper, respectively. Clearly, droplets are observed only in the presence of solvent. The spray process was monitored using a 30 Hz camera and details are shown in Figure S1 and the Supporting Information videos. Note that there are similarities to the experiments described by Pagnotti and co-workers.^{15,16}

Computational Resources. All programs used in the simulation of zero volt PS were coded in Python 3.4.2 and computed using computational resources provided by Information Technology at Purdue Research Computing (RCAC) on the Carter supercomputer. Smaller codes were tested on a small desktop computer (core i3).

Instrumentation. Mass spectra were acquired using a Thermo Fisher LTQ mass spectrometer (Thermo Scientific Inc., San Jose, CA). The MS inlet capillary temperature was kept between 150 and 200 °C except where noted, and the tube lens voltage and the capillary voltage were held at zero volt for both positive and negative ion detection. Collision-induced dissociation (CID) was used to carry out tandem mass spectrometry analysis on precursor ions mass-selected using windows of 1.5 mass units. To record the corresponding kV PS spectra, 3.5 kV and 2.0 kV were used in the positive and negative ion modes, respectively, while for nESI 1.5 kV was used in both polarities. The same CID conditions were used for the analysis of the same sample regardless of the ionization method.

RESULTS AND DISCUSSION

Characteristics of Zero Volt PS Mass Spectra. A variety of samples was used to test the ionization capabilities of zero volt PS. As shown in Figure 2, both positive and negative

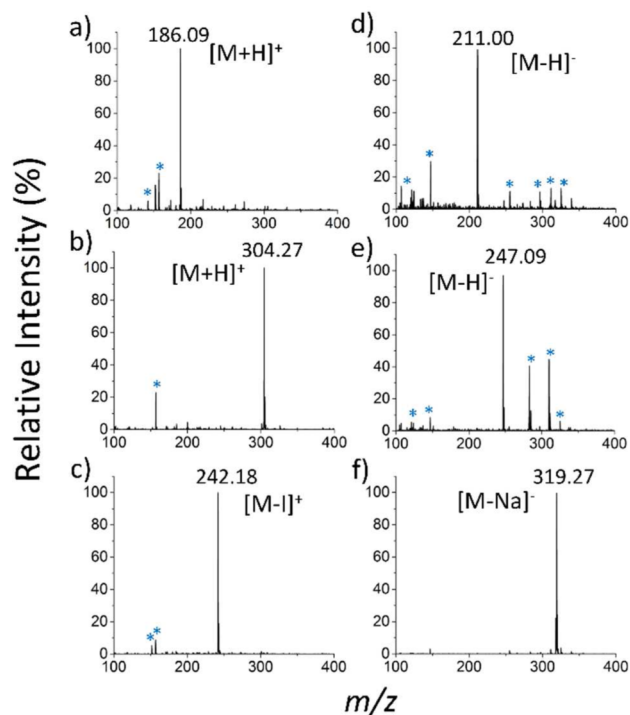


Figure 2. Mass spectra recorded using zero volt PS of three samples examined in the positive ion mode: a) 1 ppm tributylamine; b) 8 ppm cocaine, and c) 1 ppm tetrabutylammonium iodide and three samples examined in the negative ion mode: d) 10 ppm 3,5-dinitrobenzoic acid, e) 10 ppm fludiononil, and f) 10 ppm sodium tetraphenylborate. Methanol and water (v/v 1:1) were used as spray solvent for all samples. Both positive and negative signals were recorded with much lower intensities compared with kV PS and nESI. * Indicates the presence of background species.

spectra were obtained, although the signal intensities were about 2 orders of magnitude lower than those of nESI and kV PS spectra. The MS/MS results for zero volt PS were almost identical to those for the same ions generated by nESI and kV PS (Figures S2 and S3). These results show that the range of analytes to which zero volt PS is applicable is very similar to kV PS and nESI, but the ionization efficiency is much lower.

As noted at the beginning of the paper, ionization without application of a voltage has been observed using several methods. This makes it important to seek to understand the fundamental processes that lead to the formation of ions at zero volts. It is expected that such an enquiry for zero volt PS might be of some later use in guiding mechanistic studies of the other methods. A simple experiment was performed to determine the maximum distance between the paper and MS inlet that still allows observation of signal. It was found that without external forces and with the instrument and paper used, the paper must be within 1 mm of the inlet for the observation of a spray and the corresponding ion signal. At larger distances, an external force such as an applied voltage or additional pneumatic force is needed. A distance of 0.3–0.5 mm was chosen for subsequent experiments to optimize signal intensity and lower its fluctuations. The spray process was monitored using a 30 Hz

camera in an experiment that used 50 ppm of tributylamine fed continuously onto the paper at a flow rate of 15 $\mu\text{L}/\text{min}$. The emission of individual droplets occurs rapidly enough that the chronogram appears to be continuous when observed using an ion injection time of 100 ms (Figure S1f). By illuminating the spray with a hand-held red laser pointer the spray process could be videographed. Figure S1 a-d shows the suction of one droplet over the course of 4 consecutive images. This indicates that a single suction event occurs in a time on the order of ~ 100 ms. This experiment was repeated using manual additions of solvent (7 μL), and similar droplet events are observed. Movies of the continuous and discrete methods of analysis are included in the Supporting Information. The important finding is that signal is observed only when a droplet event is recorded by the camera, indicating that droplets are necessary to produce gas phase ions.

Source of Protons, pH Effect, and Low Voltage Effect. Figure 3 shows the zero volt PS spectrum of 1 ppm

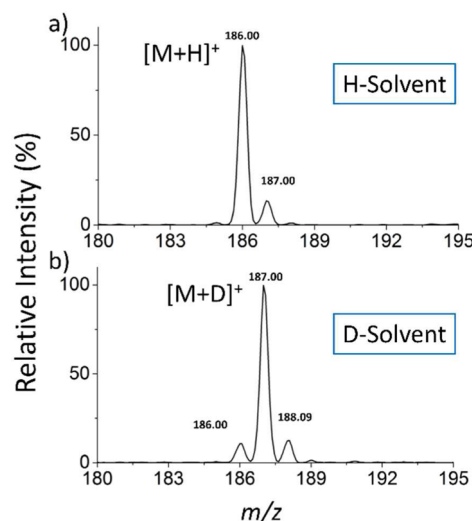


Figure 3. Zero volt PS mass spectra of 1 ppm tributylamine using a) methanol/water (v/v 1:1) and b) deuterated methanol/water (v/v 1:1) as solvent. When deuterated solvent is used, $[M + D]^+$ becomes the major peak.

tributylamine using methanol:water 1:1 and deuterated methanol:water 1:1 as solvents, respectively (Figure 3a and 3b). When methanol/water was used, m/z 186 ($[M + H]^+$) was the dominant peak, accompanied by an isotopic signal at m/z 187. However, when deuterated methanol/water was used, m/z 187, $[M + D]^+$, was dominant, and m/z 188 is its isotopic peak. These results indicate that the protons mainly come from the solvent and that the normal acid/base equilibria occurring in bulk solution are ultimately responsible for the ions seen in the mass spectra. In Figure 3b, there is still a small peak of m/z 186, while in Figure 3a ions of m/z 185 are virtually absent, indicating that a small proportion of tributylamine is still ionized as $[M + H]^+$ when deuterated solvents are used. Possible sources of the proton include autoionization ($2 M \rightleftharpoons [M + H]^+ + [M - H]^-$), gas phase water molecules, and residual protic compounds in the instrument.

The effects of solvent pH on the spectra have been tested using a representative compound, tributylamine. The intensity of the signal for the protonated molecule is high at pH 7, but when the pH is raised to 10, the intensity drops to zero. Further tests were done by using a series of aromatic heterocyclic

compounds (pyridine, guanine, thymine, and adenine) at neutral and acidic pH (Figure S4). The results show that all four compounds ionize well from acidic solution; pyridine and adenine also ionize at neutral pH, while guanine and thymine do not. These observations are consistent with expectations based on acid/base solution equilibria. The pK_a values of the conjugate acids of thymine and guanine are 0 and 3.2, respectively, while the pyridine and adenine values are significantly higher, 5.25 and 4.1, respectively.³⁰ A series of basic amines including tetramethyl-1,4-butanediamine, diisopropylamine, and methyl amine was also analyzed to investigate the effect of proton affinity (Figure S5). Tetramethyl-1,4-butanediamine has the highest proton affinity (1046.3 kJ/mol) among these analytes and also the highest absolute MS signal intensity. Diisopropyl amine (971.9 kJ/mol) is second in PA, and methyl amine (899 kJ/mol) has the lowest PA and MS signal. Basicity in the gas phase and in solution appear to play important roles in determining the types of ions and conditions (pH) under which they will be observed, similar to the effects observed in electrospray.³¹

To investigate the role low - as opposed to zero - voltages can have on ionization, paper spray experiments were performed using diphenylamine and low and zero volts. The results demonstrate that the small signal at zero volts rises measurably (by a factor of 1.5) upon providing 1 V on the paper (Figure S6) and increases by a factor of 2.5 on raising the potential to 10 V (data not shown). The addition of even a low voltage supplies additional charges, which increases ionization efficiency.

Analyzing Organic Salt/Organic Analyte Mixtures by Zero Volt PS, kV PS, and nESI. A mixture containing 9 ppm cocaine and 0.1 ppm tetrabutylammonium iodide was examined by nESI, kV PS, and zero volt PS. The results are shown in Figure 4a-c. For nESI and kV PS, cocaine (protonated molecule, m/z 304) is the dominant peak, while the signal intensity of tetrabutylammonium (m/z 242) is only about 2% of that of cocaine. For zero volt PS, m/z 304 is still dominant, but the relative intensity of tetrabutylammonium (m/z 242) is much higher than in nESI and kV PS (about 50% relative abundance). The trend is even more obvious in the results of 9 ppm morphine/0.1 ppm tetrabutylammonium iodide (Figure S7a,b,c). The data for nESI (Figure S7a) and kV PS (Figure S7b) show the signal for morphine (m/z 286) to be the base peak, while the relative abundance of tetrabutylammonium (m/z 242) is only about 2% in both cases. By contrast, in the zero volt PS result, it is the ion m/z 242 that constitutes the base peak, while the relative abundance of the protonated morphine ion is only about 10% (Figure S7c). An analogous effect was observed in the negative ion mode, by analyzing a mixture of 36 ppm sodium tetraphenylborate and 3,5-dinitrobenzoic acid (Figure S7 d,e,f).

To account for these results we note the well-known fact both in nESI and in conventional kV PS that the signal intensity is closely related to the concentration of the analyte, at least in the lower concentration range where the available number of charges is sufficient to convert all analyte into the ionic form. The observation that zero volt PS is ca. 2 orders of magnitude less efficient than kV PS and nESI is interpreted simply as the result of the limited number of charges provided by the statistical droplet breakup process versus direct solvent charging. However, this does not explain the large differences between the cocaine/tetrabutylammonium and morphine/tetrabutylammonium ion signals in zero volt PS vs the

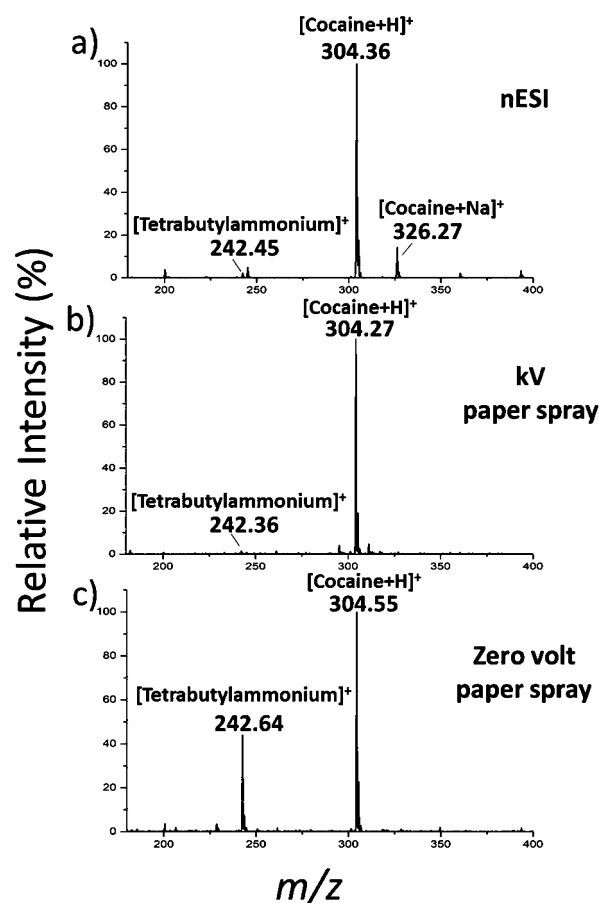
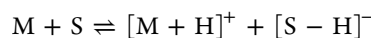
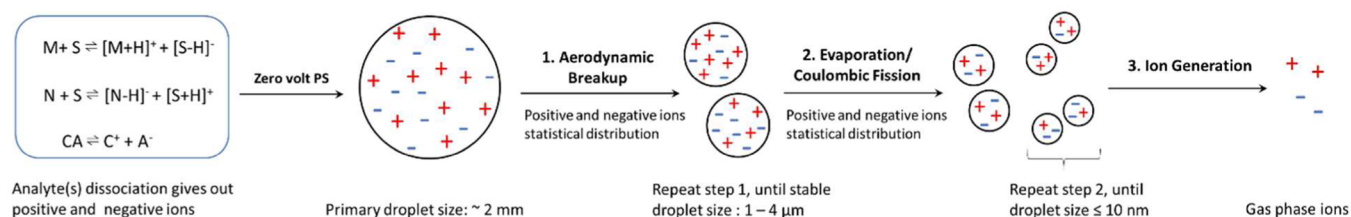


Figure 4. Mass spectra of a mixture of 9 ppm cocaine and 0.1 ppm tetrabutylammonium iodide using a) nESI, b) kV PS, and c) zero volt PS.

conventional PS and nESI methods. The aqueous pK_b of cocaine is 5.39 (15 °C), and morphine is slightly higher, 5.79 (25 °C). This means that morphine should produce somewhat fewer ions than cocaine even when their absolute concentrations are the same. However, the main reason for the low relative intensity of morphine in zero volt PS is likely the lower surface activity of morphine compared to cocaine.³² Evidence for this comes from the fact that when mixed with the very surface active compound tetrabutylammonium iodide, suppression of ionization is much more obvious for morphine than for cocaine in zero volt PS. In kV PS and nESI, the influence of surface activity is not as severe as in zero volt PS since their ionization efficiencies are so high that most of the analytes in the droplets can be ionized and pushed to the droplet surface. A parallel result is observed in negative ion mode where the surface active tetraphenylborate signal is relatively enhanced in zero volt PS as compared to the kV PS and nESI experiments. Given these qualitative explanations we can now test them using a quantitative model of the ionization mechanism.

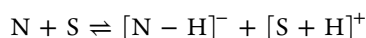
Overview of Ionization Mechanism for Zero Volt PS. It is well-known that most analytes that can be ionized by ESI (or nESI) or by PS are Bronsted acids or bases. For a basic compound M dissolved in a solvent (S), a certain amount of M exists in the ion pair form (normally as solvent-separated ion pairs) because of the equilibrium:



Scheme 1. Overview of the Ionization Mechanism of Zero Volt PS Ionization Including Representations of the Aerodynamic Breakup Process and the Droplet Evaporation/Coulombic Fission^a


^aIn both steps statistical distribution of charge to the fragments is assumed.

For negative ion generation from of an acidic compound N, the equilibrium is



For an ionic compound, say CA, there exists a dissociation equilibrium:



It is these solution-phase ion pairs which can go on to be evaporated and detected in zero volt PS as positively or negatively charged ions.

In zero volt PS, a droplet experiences aerodynamic forces as it is pulled into the mass spectrometer by the suction of the vacuum system. These aerodynamic forces break apart droplets until they reach a size on the order of 1 to 4 μm where the aerodynamic forces are no longer strong enough to cause further droplet breakup.^{29,33} Aerodynamics forces are described by the Weber number, which is defined as

$$We = \frac{\rho_g (V_g - V_d)^2 D_d}{\sigma} \quad (1)$$

where ρ_g is the gas density, V_g is the gas velocity, V_d is the droplet velocity, D_d is the diameter of the droplet, and σ is the surface tension of the solvent.³⁴ The droplet will continue to break up while its Weber number is larger than 10 (Figure S8).^{34,35} During the aerodynamic breakup process, there is a very large chance that the positive charges and negative charges will be unevenly separated, that is to say, many of these progeny droplets will be (slightly) charged. The extent of charging is unknown. However, because the initial Weber number in zero volt paper spray is larger than 1000 a catastrophic breakup of the initial droplet occurs to produce progeny droplets (Figure S8).^{34,36} After aerodynamic breakup it is assumed that droplets will undergo multiple rounds of evaporation and Coulombic fission until they are ionized by either of the main ESI models, the charge residue model or the ion evaporation model^{37,38} or its close analog, solvated ion emission.²⁶ A schematic of the overall mechanism is shown in Scheme 1. The model used here to describe evaporation and fission is similar to other approaches used to model nESI based on Monte Carlo methods,³⁹ except that droplet charging is determined by nonsymmetrical fragmentation as described by Dodd.²⁸ While the charging calculated by Dodd is small,^{28,40} there is enough charge to allow for the Coulombic fission of most 1 to 4 μm droplets to occur after an appropriate evaporation time. Note, too, that we assume statistical breakup and resulting charge distributions in the fragments during the early aerodynamic phase of bulk breakup but are aware of the fact that this is simply a first approximation. Simulations have been done based on the above postulated mechanism. The initial concentration

and diameter for each droplet were specified, but the charge of each droplet was randomly assigned based on a theory described by Dodd.²⁸ To determine the initial charge, the number of ions an analyte forms in solution was calculated based on the initial concentration and dissociation constant of the analyte. Statistical fluctuations in the number of positive and negative ions in each droplet were modeled by a binomial distribution

$$f(z; n, p) = \binom{n}{z} p^z (1 - p)^{n-z} \quad (2)$$

where p is the probability of an ion being charged (either positive or negative), n is the number of ions, and z is number of positive charges. The difference in ion polarity count determines the initial charge. It should be noted that charge is assumed to be carried only by analytes added to the solution. The droplet then evaporates until its diameter reaches the Rayleigh limit (3).^{38,41}

$$D_R = \left(\frac{D_q^2 * e^2}{(\pi^2 * 8 * \epsilon_0 * \sigma)} \right)^{1/3} \quad (3)$$

Here D_R is the diameter of the droplet at the Rayleigh limit, D_q is the charge on the droplet, e is elementary charge, ϵ_0 is the permittivity of a vacuum, and σ is the solvent surface tension.

At the Rayleigh limit a droplet undergoes fission and produces progeny droplets. Accordingly the size of precursor and progeny droplets was calculated according to these equations

$$D_d = (1 - \Delta m)^{1/3} * D_R \quad (4)$$

$$D_{pD} = \left(\frac{\Delta m}{N_{pd}} \right)^{1/3} D_R \quad (5)$$

where N_{pd} is the number of progeny droplets taken to be 10, D_{pd} is the diameter of the progeny droplets, and $\Delta m = 0.02$. The number of analytes in each progeny droplet was determined from two Poisson distributions: the concentration of ions, $N_{anal-IP}$ (both positive and negative), and the concentration of free ions in the outer region of the droplet, N_{anal-q} . The position of a solvated ion within the droplet is determined by its surface activity, S . Surface activity is a number between 0 and 1 describing the probability of a molecule being at the surface or the interior of the droplet. Larger values of surface activity means the analyte competes more strongly for surface sites. Surface activity is modeled by a binomial distribution, similar to eq 2, except that $p = S$, n is the number of ions, and z is the number of ions found in the outer region of

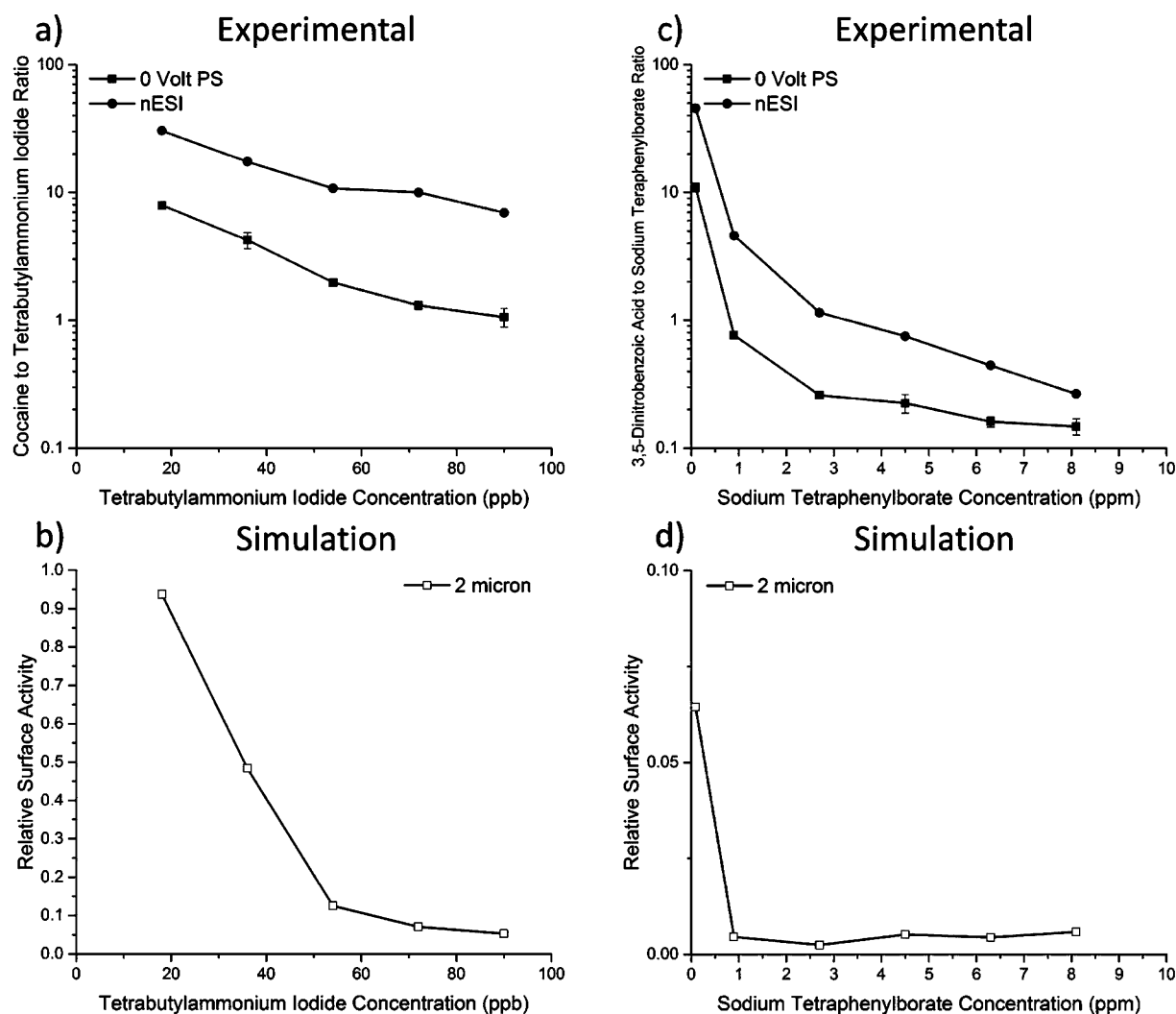


Figure 5. a) Cocaine to tetrabutylammonium cation ratio dependence in positive ion mode for zero volt PS and nESI. Cocaine concentration is held constant at 1 ppm, while tetrabutylammonium iodide concentration changes. b) The relative surface activity of cocaine calculated according to the experimental data in a). c) Ratio dependence of 3,5-dinitrobenzoate to tetraphenylborate in negative ion mode for zero volt PS and nESI. 3,5-Dinitrobenzoic acid concentration is held constant at 20 ppm, while the sodium tetraphenylborate concentration changes. d) Relative surface activity of 3,5-dinitrobenzoic acid calculated according to the experimental data in c). Surface activity of the salt is assumed to be 1 for all simulations.

the droplet.³⁹ The number of ions, $N_{\text{anal-IP}}$, and charges, $N_{\text{anal-q}}$, is chosen randomly from a Poisson distribution.

$$f(N_{\text{anal-IP}}; N_{\text{IP}}) = \frac{e^{-N_{\text{IP}}} N_{\text{IP}}^{N_{\text{anal-IP}}}}{N_{\text{anal-IP}}!} \quad (6)$$

Here N_{IP} is the average number of ions close to the surface. The same equation is used for $N_{\text{anal-q}}$ with the appropriate substitutions. For the progeny droplets, additional charging can arise from the statistical fluctuations in the number of positive and negative ions, and this is modeled in the same manner as above (2). The evaporation/Coulombic fission process continues until all droplets reach a size of 10 nm. At 10 nm, ions free of their counter charge are considered ionized (i.e., considered to undergo subsequent rapid desolvation), which is a simplification of the actual processes that leads to ion formation. Ions are produced from droplet smaller than 10 nm by the ion emission mechanism or by the charge residue model.²⁶ The formation of gas-phase ions from 10 nm droplets is not explicitly modeled here. A more detailed explanation is provided in the Supporting Information.

There are differences, but there are also strong similarities in the ionization mechanism of zero volt PS and conventional kV PS. Both processes involve the key steps of (i) droplet formation and (ii) droplet breakup. Droplet formation is mostly due to pneumatic forces in zero volt paper spray, whereas it is mostly due to electrical forces at kV paper spray. There exists a continuum in behavior between zero volt PS and kV PS as evidenced by the low voltage PS data cited above. Droplet breakup starts with a mechanical breakup process which may or may not occur in kV PS and is then followed by processes analogous to those of kV PS.

Single Analyte Simulation. Simulations were run with 2 μm droplets to investigate the possible limits of detection of zero volt PS. Both sizes lead to indicated limits of detection between 10^{-7} and 10^{-8} M (Figure S8), based on the assumption of being able to detect a single ion. The detection limit determined from simulation is calculated from the ionization efficiency, which is defined as the ratio of the number of ions generated vs the total number of molecules used.⁴² Qualitatively, 18 ppb (4.87×10^{-8} M) of tetrabutylammonium iodide could be detected experimentally,

which is in good agreement with the estimate of detectability by simulation. The simulation was also repeated at three different surface activities, and it was found that the number of ionized molecules decreases as the surface activity decreases (Figure S10). Surface activity has been reported to have a similar effect on the ionization efficiency.^{43,44}

Experimental and Simulated Results and Mechanistic Considerations for Multianalyte Mixtures. A series of mixtures of cocaine and tetrabutylammonium iodide were analyzed with zero volt PS. In Figure 5a the amount of tetrabutylammonium iodide was varied, while the amount of cocaine was held constant at 1 ppm. A similar experiment was performed using 3,5-dinitrobenzoic acid and sodium tetraphenylborate but analyzed in negative ion mode. In Figure 5c the amount of sodium tetraphenylborate was changed, while the concentration of 3,5-dinitrobenzoic acid was held constant at 20 ppm. At each point, the ratio of (de)protonated molecular ion to salt was calculated. Simulations were run in which the more surface active compound (salts in this case) was assumed to have a surface activity of 1 and surface activity of (de)protonated molecular ion relative to the salt was varied until the simulated ratio matched within 1% error of the experimental ratio.

In Figure 5a, as the amount of tetrabutylammonium iodide decreases the ratio of cocaine to tetrabutylammonium iodide increases for both zero volt PS and nESI. Note that nESI has larger ratios than zero volt PS. This is because the kV applied voltage provides protons^{38,45} which can serve to ionize the cocaine but will not cause additional ionization of the tetrabutylammonium iodide salt. Thus, the measured ratio becomes closer to the concentration ratio, with differences being due to intrinsic ionization and detection efficiency. We applied the experimental intensity ratios of zero volt PS to our simulation and calculated the relative surface activity trend. The results are shown in Figure 5b. As the amount of tetrabutylammonium iodide decreases the relative surface activity of cocaine is calculated to increase. This makes sense since as the amount of tetrabutylammonium iodide decreases more cocaine will move toward the droplet surface and can compete against the tetrabutylammonium cation for surface sites.⁴⁶ Tang et al. developed a model, which suggests that at low concentrations, 10^{-8} to 5×10^{-6} M, the ratio of analyte ion signals is dependent upon the relative surface activities of the two analytes.³² This agrees with our simulation results very well. Figure 5c,d display the same general trend observed in Figure 5a,b. As the concentration of sodium tetraphenylborate decreases the ratio of 3,5-dinitrobenzoic acid to sodium tetraphenylborate decreases (Figure 5c), while the relative surface activity of 3,5-dinitrobenzoic acid increases (Figure 5d). A similar set of experiments was performed except that the concentration of the analyte was varied, and the salt concentration was held constant (Figure S11). This produced similar conclusions, and a detailed explanation is provided in the Supporting Information.

CONCLUSION

Chemical analysis at zero volts from paper substrates has been demonstrated. Zero volt PS gives both positive and negative ion signals and allows detection of similar compounds to those seen by kV PS and nESI but with lower ionization efficiency. In spite of the low efficiency, the process is intrinsically very gentle and is more sensitive to surface active compounds. A mechanism for zero volt PS has been proposed based on the statistical

fluctuation of positive and negative ions in droplet solutions during the course of droplet breakup. This model (developed in detail in the Supporting Information) has been used to predict a detection limit similar to that observed experimentally. In the case of multiple analytes, the simulation is also able to calculate the relative surface activity of both positive and negative ions, such as cocaine and 3,5-dinitrobenzoic acid. The relationship of this model to other zero volt spray ionization mechanisms is not known but is of great future interest, especially for the inlet ionization experiments^{15,16} and the nanowire spray⁴⁷ methods. Besides the understanding of its mechanism, zero volt PS also has potential application advantages: it could be used to study systems where there is a need to avoid the influence of external electric fields and at the same time to use paper to eliminate the complex matrix, such as in living organisms analysis. In the course of this work we have learned of related unpublished paper spray ionization experiments done by Dr. Akira Motoyama of Shiseido Company.

ASSOCIATED CONTENT

Supporting Information

Additional information as noted in text. The Supporting Information is available free of charge on the ACS Publications website at DOI: 10.1021/acs.analchem.5b01225.

AUTHOR INFORMATION

Corresponding Author

*E-mail: cooks@purdue.edu.

Author Contributions

#These authors contributed equally.

Notes

The authors declare no competing financial interest.

ACKNOWLEDGMENTS

The support of the National Science Foundation CHE 1307264 is acknowledged. T.P. acknowledges DST for funding. D.S. and R.N. acknowledge UGC for their research fellowship. Yafeng Li is a visiting student from the Institute of Chemistry, Chinese Academy of Sciences, and she acknowledges the Chinese Scholarship Council for financial support.

REFERENCES

- (1) Takáts, Z.; Wiseman, J. M.; Gologan, B.; Cooks, R. G. *Science* **2004**, *306*, 471–473.
- (2) Monge, M. E.; Harris, G. A.; Dwivedi, P.; Fernández, F. M. *Chem. Rev.* **2013**, *113*, 2269–2308.
- (3) *Ambient Ionization Mass Spectrometry*; The Royal Society of Chemistry; 2015; pp P001–508.
- (4) Schäfer, K.-C.; Balog, J.; Szaniszló, T.; Szalay, D.; Mezey, G.; Dénes, J.; Bognár, L.; Oertel, M.; Takáts, Z. *Anal. Chem.* **2011**, *83*, 7729–7735.
- (5) Blakley, C. R.; Carmody, J. J.; Vestal, M. L. *Anal. Chem.* **1980**, *52*, 1636–1641.
- (6) Blakley, C. R.; Vestal, M. L. *Anal. Chem.* **1983**, *55*, 750–754.
- (7) Hirabayashi, A.; Sakairi, M.; Koizumi, H. *Anal. Chem.* **1994**, *66*, 4557–4559.
- (8) Hirabayashi, A.; Sakairi, M.; Koizumi, H. *Anal. Chem.* **1995**, *67*, 2878–2882.
- (9) Hirabayashi, A.; Hirabayashi, Y.; Sakairi, M.; Koizumi, H. *Rapid Commun. Mass Spectrom.* **1996**, *10*, 1703–1705.
- (10) Hirabayashi, Y.; Hirabayashi, A.; Takada, Y.; Sakairi, M.; Koizumi, H. *Anal. Chem.* **1998**, *70*, 1882–1884.
- (11) Ozdemir, A.; Lin, J.-L.; Wang, Y. S.; Chen, C.-H. *RSC Adv.* **2014**, *4*, 61290–61297.

- (12) Haddad, R.; Sparrapan, R.; Eberlin, M. N. *Rapid Commun. Mass Spectrom.* **2006**, *20*, 2901–2905.
- (13) Haddad, R.; Sparrapan, R.; Kotiaho, T.; Eberlin, M. N. *Anal. Chem.* **2008**, *80*, 898–903.
- (14) Haddad, R.; Milagre, H. M. S.; Catharino, R. R.; Eberlin, M. N. *Anal. Chem.* **2008**, *80*, 2744–2750.
- (15) Pagnotti, V. S.; Inutan, E. D.; Marshall, D. D.; McEwen, C. N.; Trimpin, S. *Anal. Chem.* **2011**, *83*, 7591–7594.
- (16) Pagnotti, V. S.; Chubatyi, N. D.; McEwen, C. N. *Anal. Chem.* **2011**, *83*, 3981–3985.
- (17) Wang, B.; Trimpin, S. *Anal. Chem.* **2014**, *86*, 1000–1006.
- (18) Wu, C.-I.; Wang, Y.-S.; Chen, N. G.; Wu, C.-Y.; Chen, C.-H. *Rapid Commun. Mass Spectrom.* **2010**, *24*, 2569–2574.
- (19) Zhu, H.; Li, G.; Huang, G. J. *Am. Soc. Mass Spectrom.* **2014**, *25*, 935–942.
- (20) Chen, T.-Y.; Chao, C.-S.; Mong, K.-K. T.; Chen, Y.-C. *Chem. Commun.* **2010**, *46*, 8347–8349.
- (21) Chen, T.-Y.; Lin, J.-Y.; Chen, J.-Y.; Chen, Y.-C. *J. Am. Soc. Mass Spectrom.* **2010**, *21*, 1547–1553.
- (22) Ozdemir, A.; Lin, J.-L.; Gillig, K. J.; Chen, C.-H. *Analyst* **2013**, *138*, 6913–6923.
- (23) Wang, H.; Liu, J.; Cooks, R. G.; Ouyang, Z. *Angew. Chem., Int. Ed.* **2010**, *49*, 877–880.
- (24) Manicke, N. E.; Yang, Q.; Wang, H.; Oradu, S.; Ouyang, Z.; Cooks, R. G. *Int. J. Mass Spectrom.* **2011**, *300*, 123–129.
- (25) Espy, R. D.; Teunissen, S. F.; Manicke, N. E.; Ren, Y.; Ouyang, Z.; van Asten, A.; Cooks, R. G. *Anal. Chem.* **2014**, *86*, 7712–7718.
- (26) Konermann, L.; Ahadi, E.; Rodriguez, A. D.; Vahidi, S. *Anal. Chem.* **2013**, *85*, 2–9.
- (27) Narayanan, R.; Sarkar, D.; Cooks, R. G.; Pradeep, T. *Angew. Chem., Int. Ed.* **2014**, *53*, 5936–5940.
- (28) Dodd, E. E. *J. Appl. Phys.* **1953**, *24*, 73–80.
- (29) Zilch, L. W.; Maze, J. T.; Smith, J. W.; Ewing, G. E.; Jarrold, M. F. *J. Phys. Chem. A* **2008**, *112*, 13352–13363.
- (30) Yen, T.-Y.; Judith Charles, M.; Voyksner, R. D. *J. Am. Soc. Mass Spectrom.* **1996**, *7*, 1106–1108.
- (31) Ehrmann, B. M.; Henriksen, T.; Cech, N. B. *J. Am. Soc. Mass Spectrom.* **2008**, *19*, 719–728.
- (32) Tang, L.; Kebarle, P. *Anal. Chem.* **1993**, *65*, 3654–3668.
- (33) Wang, R.; Allmendinger, P.; Zhu, L.; Gröhn, A.; Wegner, K.; Frankevich, V.; Zenobi, R. *J. Am. Soc. Mass Spectrom.* **2011**, *22*, 1234–1241.
- (34) Krzeczkowski, S. A. *Int. J. Multiphase Flow* **1980**, *6*, 227–239.
- (35) Wierzba, A. *Exp. Fluids* **1990**, *9*, 59–64.
- (36) Pilch, M.; Erdman, C. A. *Int. J. Multiphase Flow* **1987**, *13*, 741–757.
- (37) Iribarne, J. V.; Thomson, B. A. *J. Chem. Phys.* **1976**, *64*, 2287–2294.
- (38) Kebarle, P.; Verkerk, U. H. *Mass Spectrom. Rev.* **2009**, *28*, 898–917.
- (39) Hogan, C. J., Jr.; Biswas, P. *J. Am. Soc. Mass Spectrom.* **2008**, *19*, 1098–1107.
- (40) Knochenmuss, R. *Mass Spectrometry* **2013**, *2*, S0006–S0006.
- (41) Rayleigh, L. *Philos. Mag. Ser. 5* **1882**, *14*, 184–186.
- (42) Murray, K. K.; Boyd, R. K.; Eberlin, M. N.; Langley, G. J.; Li, L.; Naito, Y. *Pure Appl. Chem.* **2013**, *85*, 1515–1609.
- (43) Cech, N. B.; Enke, C. G. *Anal. Chem.* **2000**, *72*, 2717–2723.
- (44) Cech, N. B.; Enke, C. G. *Mass Spectrom. Rev.* **2001**, *20*, 362–387.
- (45) Kertesz, V.; Van Berkel, G. J. *Anal. Chem.* **2007**, *79*, 5510–5520.
- (46) Enke, C. G. *Anal. Chem.* **1997**, *69*, 4885–4893.
- (47) Narayanan, R.; Sarkar, D.; Som, A.; Cooks, R. G.; Pradeep, T. **2015**, Unpublished.